The extracellular matrix molecule tenascin C modulates expression levels and territories of key patterning genes during spinal cord astrocyte specification

Michael Karus[1,2], Bernd Denecke[3], Charles ffrench-Constant[4], Stefan Wiese[2,5] and Andreas Faissner[1,2,*]

SUMMARY

The generation of astrocytes during the development of the mammalian spinal cord is poorly understood. Here, we demonstrate for the first time that the extracellular matrix glycoprotein tenascin C regulates the expression of key patterning genes during late embryonic spinal cord development, leading to a timely maturation of gliogenic neural precursor cells. We first show that tenascin C is expressed by gliogenic neural precursor cells during late embryonic development. The loss of tenascin C leads to a sustained generation and delayed migration of *Fgfr3*-expressing immature astrocytes in vivo. Consistent with an increased generation of astroglial cells, we documented an increased number of GFAP-positive astrocytes at later stages. Mechanistically, we could demonstrate an upregulation and domain shift of the patterning genes Nkx6.1 and Nkx2.2 in vivo. In addition, sulfatase 1, a known downstream target of Nkx2.2 in the ventral spinal cord, was also upregulated. Sulfatase 1 regulates growth factor signalling by cleaving sulphate residues from heparan sulphate proteoglycans. Consistent with this function, we observed changes in both FGF2 and EGF responsiveness of spinal cord neural precursor cells. Taken together, our data implicate Tnc in the regulation of proliferation and lineage progression of astroglial progenitors in specific domains of the developing spinal cord.

KEY WORDS: Spinal cord, Gliogenesis, Tenascin C, Extracellular matrix, Growth factor responsiveness, Neural patterning

INTRODUCTION

Astrocytes are the most abundant cell type in the adult central nervous system (CNS). Despite their various roles in CNS function and homeostasis (for reviews, see Barres, 2008; Faissner et al., 2010; Haydon, 2001) their ontogenetic development remains poorly understood.

Generally, it is known that the development of the CNS is a sequential process, in which neural precursor cells (NPCs) first generate neurons (neurogenesis) and later generate glial cells, namely oligodendrocytes and astrocytes (gliogenesis) (Temple, 2001). This shift in cell type specification is accompanied by a shift in growth factor responsiveness of NPCs. While NPCs primarily respond to fibroblast growth factor 2 (FGF2) during neurogenesis, they acquire an epidermal growth factor (EGF)-responsiveness at the onset of gliogenesis owing to a sustained FGF2 signalling (Lillien and Raphael, 2000). Thus, EGF responsiveness can be considered to be a hallmark of gliogenesis during CNS development (Temple, 2001). Gliogenesis begins around E12.5 in the mouse spinal cord with the specification of oligodendrocyte precursor cells (OPCs) from the former motoneuron progenitor domain (Rowitch et al., 2002). At the same time, fibroblast growth factor receptor 3 (FGFR3)-positive astrocyte precursor cells appear in the other domains of the ventricular zone (VZ) (Pringle et al., 2003). These domains, distinguished by a defined expression of homeodomain transcription factors, give rise to different astrocyte subpopulations in the developing spinal cord (Deneen et al., 2006; Hochstim et al., 2008; Muroyama et al., 2005).

The regulatory mechanisms that underlie the biology of NPCs during development in terms of proliferation and differentiation have been analysed extensively during the past years. Our laboratory has contributed to the understanding of extracellular matrix (ECM) molecules for the regulation of NPC behaviour (Czopka et al., 2010; Czopka et al., 2009; Garwood et al., 2004; Sirko et al., 2009; Sirko et al., 2010; Sirko et al., 2007; von Holst et al., 2007; von Holst et al., 2006). One particular ECM molecule is the glycoprotein tenascin C. (In this article, *Tnc* refers to the gene or the mRNA and Tnc refers to the protein or to general statements.) During CNS development Tnc is transiently expressed in the brain by radial glia cells (Gotz et al., 1998; Stoykova et al., 1997; von Holst et al., 2007). In the adult CNS, Tnc remains expressed by neurogenic subventricular zone astrocytes, but becomes strongly upregulated upon CNS lesions by reactive astrocytes, and it appears to affect the glial acidic fibrillary protein (GFAP) expression levels (Brodkey et al., 1995; Camand et al., 2004; Chen et al., 2010; Kazanis et al., 2007; Laywell et al., 1992; Robel et al., 2011; Robel et al., 2009; Steindler et al., 1995).

Although much is known about the role of Tnc in astrocyte biology under pathological conditions, its possible influence on astrogliogenesis during CNS development has not yet been analysed. In this study, we show for the first time that Tnc is expressed by a subset of gliogenic precursors in the developing mouse spinal cord. The loss of Tnc results in an increased generation but delayed migration of *Fgfr3* expressing immature astrocytes in vivo. Based on a whole genome expression profiling, we also show an upregulation of the homeodomain transcription

[1]Department for Cell Morphology and Molecular Neurobiology, Ruhr-University Bochum, Universitätsstraße 150, 44780 Bochum, Germany. [2]International Graduate School of Neuroscience, Ruhr-University Bochum, Universitätsstraße 150, 44780 Bochum, Germany. [3]IZKF Aachen, RWTH Aachen, 52074 Aachen, Germany. [4]Medical Research Council Centre for Regenerative Medicine and Multiple Sclerosis Society Translational Research Centre, Centre for Inflammation Research, The Queen's Medical Research Institute, University of Edinburgh, Edinburgh EH16 4TJ, UK. [5]Group for Molecular Cell Biology, Ruhr-University Bochum, Universitätsstraße 150, 44780 Bochum, Germany.

*Author for correspondence (andreas.faissner@ruhr-uni-bochum.de)

factors Nkx6.1, Nkx2.2 and of the Nkx2.2 downstream target sulfatase 1 (Sulf1). In line with this, Tnc-deficient NPCs display alterations in responsiveness towards FGF2 and EGF.

MATERIALS AND METHODS

Animals
Experiments were performed using timed-mated pregnant *Tnc* knockout mutants (Forsberg et al., 1996) and *Pax6*-deficient small eye (*sey*) mutants (Stoykova et al., 1996). The genotype of *Tnc* mutants was determined as previously described (Talts et al., 1999). For some experiments, wild-type NMRI mice (Charles River Laboratories, Wilmington, USA) were used. The age of the animals was determined according to the Theiler Stages. The day of the vaginal plug was considered to be embryonic day (E) 0.5.

Neurosphere culture
The lumbosacral spinal cord of the embryo was dissected using small forceps and the surrounding meninges were removed. The tissue was enzymatically digested using 30 U/ml papain (Worthington, New Jersey, USA) in MEM (Sigma-Aldrich, Munich, Germany) for about 30-45 minutes, depending on the age of the embryos. The digestion was stopped with ovomucoid, and the tissue was mechanically triturated in order to obtain a single cell suspension. Subsequently, primary NPC culture was performed as previously reported (von Holst et al., 2006). After 6 days, the number of neurospheres was determined by counting all neurospheres in the culture flask. To minimize the formation of non-clonal neurospheres, the cultures were not taken out of the incubator during the culture period (Coles-Takabe et al., 2008). For differentiation assays, single neurospheres or dissociated neurosphere cells were plated on poly-DL-ornithine/laminin-coated dishes (both 10 µg/ml) and incubated in neurosphere medium containing 1% (v/v) FCS at 37°C and 6% (v/v) CO_2 for a further 4 days.

Immunological reagents
The following primary antibodies were used in this study. The monoclonal antibodies were: anti-O4 (1:50; mouse IgM) (Sommer and Schachner, 1981), anti-nestin (1:500; mouse IgG; clone rat-401; Chemicon, Hofheim, Germany), anti-Nkx2.2 (1:100; mouse IgG; clone 74.5A5; DSHB, Iowa City, USA), anti-Nkx6.1 (1:100; mouse IgG; clone F55A10; DSHB, Iowa City, USA), anti-βIII tubulin (1:500; mouse IgG; clone SDL3D10; Sigma-Aldrich, Munich, Germany), anti-vimentin (1:300; mouse IgM; clone LN-6; Chemicon, Hofheim, Germany) and anti-GFAP (1:150; mouse IgG; clone GA5; Sigma-Aldrich, Munich, Germany). The polyclonal antibodies were: anti-GLAST (1:1000; guinea pig; Chemicon, Hofheim, Germany), anti-NF1α (1:1000; rabbit; Abcam, Cambridge, UK), anti-GFAP (1:300; rabbit; Dako, Hamburg, Germany), anti-EGFR (1:300; rabbit; Santa Cruz, Hamburg, Germany) and anti-Tnc (1:300; rabbit; batch Kaf14/1) (Faissner and Kruse, 1990).

Immunohistochemistry
Adult (P40) mice were deeply anesthetised with 7.5 mg/g bodyweight urethane [10% (w/v) in 0.9% (w/v) NaCl-solution] and transcardially perfused with PBS at 4°C followed by 4% (w/v) paraformaldehyde (PFA) at 4°C. Afterwards, the vertebral column at the lumbar level, including the spinal cord, was dissected, and the tissue was further processed.

Pregnant animals were killed by cervical dislocation and the embryos were removed. The trunks of the embryos were washed in PBS and fixed in PFA at 4°C for 6-24 hours depending on their age. The following day the trunks were transferred to 20% (w/v) DEPC-treated sucrose for 1 day and then embedded using TissueTec Freezing medium (Jung, Nussloch, Germany). The tissue was finally cut into 16 µm cryosections using a cryostat CM3050S (Leica, Solms, Germany). The sections were stored at –70°C until further use. For immunohistochemistry, the sections were blocked for 1 hour at room temperature in PBT1 [PBS, 1% (w/v) BSA and 0.1% (v/v) Triton X-100)/1.7% (w/v) NaCl PBS (1:1) and 10% (v/v) normal goat serum]. Thereafter, the primary antibody was incubated overnight at 4°C in PBT1 and 5% (v/v) normal goat serum. The next day the slides were washed three times with PBS followed by incubation with either Cy3- or Cy2-coupled species-specific secondary antibodies (Dianova, Hamburg,

Germany) diluted in PBS/A [PBS + 0.1% (w/v) BSA] at room temperature for 2 hours. Bisbenzemid ($1:10^5$) (Sigma-Aldrich, Munich, Germany) was included to visualize the nuclei. For 5-bromo-2′-deoxyuridine (BrdU) incorporation analysis, pregnant female mice were injected with 100 µg/g bodyweight BrdU. After 24 hours the animals were sacrificed and the embryos were processed as described above. After 15 minutes boiling in 10 mM citrate buffer (pH 6) for antigen retrieval, the immunodetection was carried out using the BrdU-labelling and detection Kit I (Roche, Mannheim, Germany) according to the manufacturer's instructions.

Immunocytochemistry
For the characterisation of freshly dissociated spinal cord cells, the tissue was digested in the same way as for neurosphere culture. Freshly dissociated cells were allowed to adhere to the culture dish for 2 hours. This recovery time frame proved to be sufficient for the detection of extracellular epitopes. After removal of the culture medium, adherent cells were washed twice with PBS/A and afterwards fixed with 4% (w/v) PFA for 10 minutes at room temperature. After fixation, the cells were washed twice with PBT1, and the incubation with the primary antibody diluted in PBT1 was performed for 30 minutes at room temperature. To detect extracellular (Tnc) or membrane-bound epitopes (O4), the incubation with the primary antibody in PBS/A was carried out before fixation for 20 minutes at room temperature. After incubation with the primary antibody, the cells were washed again with PBT1 and the incubation with either Cy3- or Cy2-coupled species-specific secondary antibodies diluted in PBS/A was carried out at room temperature for 30 minutes. Bisbenzemid ($1:10^5$) was additionally added to visualize the nuclei. Finally, the cells were washed twice with PBS and mounted in PBS/glycerine (2:1).

In situ hybridisation
Probes against *Tnc* (Czopka et al., 2009), *Pdgfra* (Czopka et al., 2009), *Fgfr3* (Pringle et al., 2003) and *Sulf1* were produced with the RNA-labelling kit (Roche, Mannheim, Germany) according to the manufacturer's instructions. The *Sulf1* probe was generated by cloning a 1186 bp fragment (nucleotides 2491-3676) into the pCRII-TOPO plasmid. In situ hybridization was performed following a published protocol (Pringle et al., 1996) on 16 µm cryosections of immersion-fixed embryonic mouse trunks.

Affymetrix GeneChip analysis
Gene expression in E15.5 lumbar spinal cord tissue of Tnc wild-type and Tnc-deficient embryos was analyzed by Affymetrix GeneChip MouseGene1.0 ST in independant triplicates. Total RNA was isolated using the RNeasy Mini Kit (Qiagen, Hilden, Germany) and quantified (Nanodrop), and the quality was assessed using RNA NanoChips with the Agilent 2100 Bioanalyzer (Agilent, USA). Probes for the GeneChip Mouse Gene 1.0 ST Arrays (Affymetrix, USA) were prepared and hybridized to the arrays according to the Ambion whole transcript expression and the Affymetrix whole transcript terminal labelling and control kits' manuals. The image data were analyzed with Affymetrix GeneChip Command Console Software (AGCC) (Affymetrix, USA). The microarray expression analysis and comparison was undertaken using Bioconductor1 packages under R2 background correction (Gentleman et al., 2004). Normalization was performed using the RMA algorithm (Irizarry et al., 2003). Only those genes with signal intensity more than threefold higher than the mean of all negative controls (n=5222) in at least one treatment condition were considered to be truly expressed and were used for further analysis. Owing to the Tnc expression levels (about 10% Tnc-expressing cells) at that age, we considered 2log regulation values of around ≥ 0.2 or ≤ -0.2 as potentially meaningful. The data discussed in this publication have been deposited in NCBI's Gene Expression Omnibus and are accessible through GEO Series accession number GSE33091.

RT-PCR
Total RNA from tissue samples was isolated using the RNeasy Mini Kit (Qiagen, Hilden, Germany) following the manufacturer's instructions. Total RNA (1 µg) was reverse transcribed using the First Strand cDNA Synthesis Kit (Fermentas, St Leon-Rot, Germany) and 1 µg cDNA was subjected to PCR analysis using the following primer pairs: *Gapdh* forward, 5′-CAAGGTCATCCATGACAACTTTG-3′; *Gapdh* reverse, 5′-GTCCAC-

CACCCTGTTGCTGTAG-3′ (28 cycles); *Nkx2.2* forward, 5′-TAAGAG-
CCCTTTCTACGACAGC-3′; *Nkx2.2* reverse, 5′-CTGACCAAGACCGG-
CACT-3′ (34 cycles); *Sulf1* forward, 5′-GCGCTTGGTGCCAGCAGAGA-
3′; *Sulf1* reverse, 5′-GGCTGCTCCACACGGGACAC-3′ (32 cycles).

Documentation and data analysis
Pictures were taken at the Axioplan2 with the AxioCam HRc camera using
the AxioVision 4.4 and 4.5 software (Zeiss, Jena, Germany). For
quantitative analysis of immunocytochemical antigen detections, a
minimum of 200 Bisbenzemid-positive nuclei were counted in at least three
independent experiments per antibody and culture condition.

For in vivo quantification, at least six sections per embryo were
analysed. To exclude any differences that were due to different rostrocaudal
levels, we used the embryonic kidneys as a landmark. Because these organs
are bilateral, this also allowed us to check whether the sections were tilted
in the sagittal plane.

To quantify the neurosphere formation from *Tnc*-deficient cells, the
number of all neurospheres in the whole culture flask was counted, and the
genotype of the embryos was determined afterwards in order to ensure
unbiased counting. The diameter of single neurospheres was measured
using ImageJ v1.41.

The data are expressed as mean±s.d. After checking for Gaussian
distribution (mean<2σ), statistical significance was assessed using the
paired and unpaired two-tailed Student's *t*-test and the *P*-values are given
as *$P \leq 0.05$, **$P \leq 0.01$ and ***$P \leq 0.001$.

RESULTS
Tnc is expressed during gliogenesis in the developing spinal cord
Tnc is transiently expressed during development of the CNS and
becomes re-expressed by reactive astrocytes, e.g. upon spinal cord
lesion (Camand et al., 2004). However, there are no precise data
available concerning the embryonic Tnc expression within the
spinal cord. Therefore, we started analysing the expression pattern
of Tnc on both mRNA and protein level in the embryonic lumbar

spinal cord. *Tnc*-expressing cells appeared at E13.5 (Fig. 1A,D)
around the central canal and in the ventral white matter.
Nevertheless, the overall expression was still very weak. Between
E13.5 and E15.5 *Tnc* became strongly upregulated. Note the strong
immunoreactivity as well as the number of *Tnc*-expressing cells in
the ventral spinal cord in comparison with the dorsal part. In
addition, the roof plate, which contains several ECM molecules at
that age (Snow et al., 1990), lacked any immunoreactivity. Finally,
we observed several *Tnc*-expressing cells at the central midline and
some cells appeared to migrate towards the pial surface owing to
their radial arrangement (Fig. 1B,E; 1B, inset). At E18.5 Tnc
expression was even stronger, especially in the future white matter.
By contrast, *Tnc*-expressing cells were absent from the region
around the central canal, which was consistent with the lack of Tnc
immunoreactivity in that area (Fig. 1C,F; 1C, inset).

Tnc is expressed within the astroglial lineage
Recently, the antigenic profiles of NPCs in the developing rat spinal
cord have been described (Barry and McDermott, 2005). Based on
this study, we compared Tnc expression with the NPC markers
nestin, glutamate/aspartate transporter (GLAST) and vimentin, and
with the astrocyte marker GFAP. Immunocytochemical analysis of
acutely dissociated spinal cord cells for Tnc and co-labelling for
these markers revealed that Tnc was expressed by NPCs and GFAP-
positive astrocytes in the developing spinal cord (Fig. 1G-J). The
quantitative data are summarized in Table 1. The relative number of
Tnc-expressing cells increased approximately eightfold from E13.5
to E18.5. During this time, the nestin-positive population declined,
whereas the GLAST-positive and the vimentin-positive population
either increased or remained constant, respectively. Furthermore,
GFAP-positive astrocytes appeared between E15.5 and E18.5 (Table
1). The quantification of double immunoreactive cells showed that
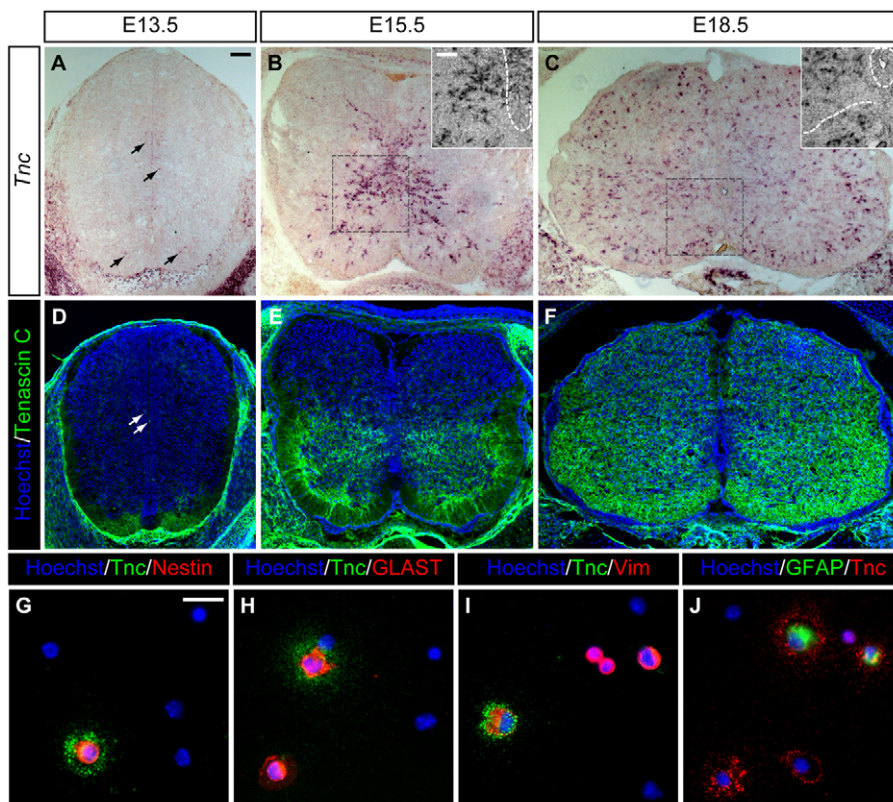the numbers of Tnc/nestin-, Tnc/GLAST- and Tnc/vimentin-positive

Fig. 1. Tnc is expressed by NPCs and astrocytes at the end of embryonic spinal cord development. (A-C) In situ hybridisation for *Tnc* on frontal spinal cord sections revealed that *Tnc*-expressing cells appeared at E13.5 at the central midline and in the developing ventral grey matter (black arrows). At E15.5, *Tnc* was expressed by cells surrounding the central canal and by cells presumably migrating to the pial surface. At 18.5, *Tnc*-expressing cells were evenly distributed throughout the grey and white matter. (D-F) Immunohistochemical detection of Tnc showed that, at E13.5, Tnc was primarily present in the developing ventral white matter and around some cells at the central canal (white arrows). At E15.5, Tnc immunoreactivity was strong in the ventral part and only weak in the dorsal part. At E18.5, Tnc was present in the whole spinal cord except for the region around the central canal. (G-J) Immunocytochemical characterisation of acutely dissociated spinal cord cells revealed that Tnc was expressed by nestin-, GLAST- and vimentin-positive cells from E13.5 onwards. At E18.5 (J), Tnc was also expressed by GFAP-positive astrocytes. Scale bars: 150 μm in A-F; 50 μm in insets; 20 μm in G-J.

Table 1. Immunocytochemical analysis of acutely dissociated spinal cord cells

Marker	E13.5	E15.5	E18.5
Tnc	2.3±0.8% (*n*=6)	9.8±3.2% (*n*=8)	15.8±4.7% (*n*=7)
Nestin	26.5±4.9% (*n*=10)	17.9±3.1% (*n*=9)	7.7±2.3% (*n*=6)
Nestin and Tnc	2.3±0.8% (*n*=6)	7.4±1.4% (*n*=4)	3.9±1.6% (*n*=3)
Tnc and Nestin/Tnc	100.0±0.0% (*n*=4)	92.1±15.8% (*n*=4)	27.3±8.8% (*n*=3)
Tnc and Nestin/Nestin	10.3±4.3% (*n*=4)	41.4±14.9% (*n*=4)	53.4±11.9% (*n*=4)
GLAST	9.1±2.4% (*n*=4)	13.6±1.9% (*n*=4)	32.3±2.1% (*n*=4)
GLAST&Tnc	2.9±1.0% (*n*=4)	7.2±1.3% (*n*=4)	11.5±2.1% (*n*=4)
Tnc and GLAST/Tnc	100.0±0.0% (*n*=4)	98.1±3.9% (*n*=4)	94.2±7.3% (*n*=4)
Tnc and GLAST/GLAST	33.0±13.1% (*n*=4)	53.4±11.9% (*n*=4)	35.6±4.5% (*n*=3)
Vimentin	28.5±9.5% (*n*=3)	22.9±6.0% (*n*=3)	25.7±4.9% (*n*=2)
Vimentin and Tnc	2.8±1.0% (*n*=3)	8.1±2.1% (*n*=3)	7.4±0.4% (*n*=2)
Tnc and Vimentin/Tnc	100.0±0.0% (*n*=4)	97.4±4.4% (*n*=4)	66.9±16.1% (*n*=2)
Tnc and Vimentin/Vimentin	11.2±6.6% (*n*=3)	35.6±6.1% (*n*=3)	29.5±7.2% (*n*=2)
GFAP	ND	ND	20.0±6.5% (*n*=4)
GFAP and Tnc	ND	ND	9.3±2.9% (*n*=3)
Tnc and GFAP/Tnc	ND	ND	66.8±4.0% (*n*=3)
Tnc and GFAP/GFAP	ND	ND	100.0±0.0% (*n*=3)

Data are mean±s.d.

cells were low at E13.5 but increased during the next days to the same extent. At E18.5, the amount of Tnc/nestin-positive cells decreased again, whereas the Tnc/GLAST-positive population and the Tnc/vimentin-positive population did not notably change between E15.5 and E18.5 (Table 1). To describe further the maturation state of Tnc-expressing cells, we additionally determined the fraction of Tnc-expressing cells among the NPC or astrocyte populations and vice versa. We found that the Tnc-positive population gradually lost the nestin and vimentin immunoreactivity. By contrast, GLAST immunoreactivity could be observed on nearly every Tnc-positive cell also at E18.5. At that stage, approximately two-thirds of the Tnc expressing cells co-expressed GFAP, indicating that the Tnc-positive population still contained several precursor cells or immature astrocytes (Table 1).

We next asked whether Tnc might be expressed within particular progenitor domains of the ventricular zone. To address this issue, we first immunohistochemically compared the Tnc expression at E15.5 with the expression of the transcription factors Nkx2.2,

Nkx6.1 and Pax6. Tnc immunoreactivity was strong around the ventral central canal, except for the most ventral part (Fig. 2A). The comparison with the above-mentioned transcription factors suggested an overlapping expression with Nkx6.1- and Pax6-positive cells (Fig. 2B-D). Indeed, colabelling of acutely dissociated E15.5 spinal cord cells for Tnc and these transcription factors confirmed the expression of Tnc by Nkx6.1- and Pax6-positive cells (Fig. 2G,H). By contrast, we did not observe Tnc/Nkx2.2 double-positive cells (Fig. 2F). Finally, we also observed Tnc/NF1α double-positive cells, demonstrating the expression of Tnc within the early astroglial lineage (Fig. 2E).

Tnc expression correlates with EGF-responsiveness and gliogenic differentiation in the embryonic spinal cord

The expression of Tnc by NPCs prompted us to characterize lumbar spinal cord NPCs grown as neurospheres at various embryonic ages with respect to growth factor responsiveness and
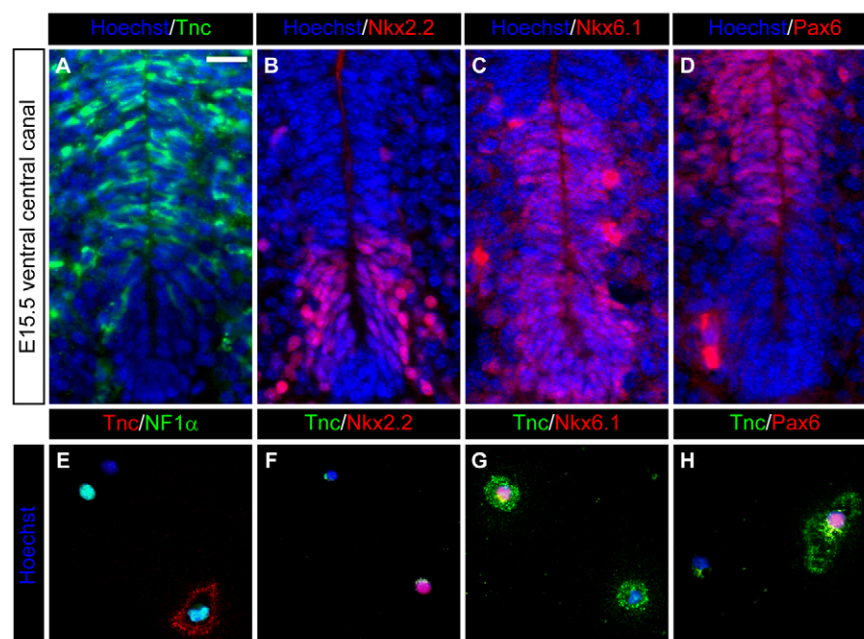

Fig. 2. Tnc is expressed within specific progenitor domains of the ventral spinal cord. (**A-D**) Immunohistochemical detection of Tnc and the transcription factors Nkx2.2, Nkx6.1 and Pax6 along the ventral part of the E15.5 spinal cord central canal suggested an overlapping expression of Tnc with Nkx6.1- and Pax6-positive cells. By contrast, the Nkx2.2 domain and the floor plate lacked any Tnc immunoreactivity. (**E-H**) Immunocytochemical characterisation of acutely dissociated E15.5 spinal cord cells indeed revealed an overlapping expression of Tnc with Nkx6.1 and Pax6. By contrast, we did not observe any Tnc/Nkx2.2-positive cells. The expression of Tnc by NF1α-positive cells clearly demonstrated its association with the astroglial lineage. Scale bar: 25 μm.

differentiation capacity. We valued the number of primary neurospheres as a relative measure of the overall growth factor responsiveness of the original tissue. The numbers are summarised in supplementary material Table S1. See supplementary material Fig. S1A for examples of neurospheres grown in the presence of either EGF or FGF2 for 6 days. During the neurogenic period from E11.5 to E13.5, the spinal cord primarily consisted of FGF2-responsive NPCs. Towards the end of neurogenesis, an EGF-responsive population emerged (supplementary material Fig. S1B). Both populations dramatically increased from E13.5 to E15.5 (supplementary material Fig. S1B). This is consistent with a previous study, demonstrating a stage-dependent increase in EGF-responsiveness in the developing cervical spinal cord (Represa et al., 2001). Interestingly, this increase coincided with the upregulation of Tnc during this period. Owing to the high Tnc expression, particularly in the ventral spinal cord at E15.5, we further dissected the spinal cord into a ventral and a dorsal part and analysed the neurosphere formation capacity from both parts separately (supplementary material Fig. S1C). Additionally, immunocytochemical analysis confirmed the higher number of Tnc-positive cells in the ventral spinal cord (supplementary material Fig. S1D). Furthermore, the ventral cell population gave rise to significantly more neurospheres than the dorsal one under both growth factor conditions (supplementary material Fig. S1E). At E18.5, the overall number of neurosphere-forming cells decreased again (supplementary material Fig. S1B).

Next, we examined the differentiation potential of single neurospheres, as well as of dissociated neurosphere cells grown from E15.5 spinal cord cells in the presence of either EGF or FGF2. Under both growth factor conditions, about 70% of the neurospheres generated a majority of astroglial cells, whereas 30%

were multipotent, as assessed by the immunocytochemical detection of GFAP, the oligodendrocyte marker O4, and the neuronal marker βIII-Tubulin. Among the neurospheres composed primarily of astrocytes, O4-positive oligodendrocytes were occasionally visible. Some contained in addition a minority of neurons (supplementary material Fig. S2A-C). However, we judged that this was not sufficient to classify the latter as truly multipotent. In parallel, we determined the differentiation capacity of dissociated neurosphere cells. The immunocytochemical analysis revealed that about 50% of the primary neurosphere cells after 4 days in culture still expressed nestin and only 10% expressed GFAP, indicative of an immature phenotype. However, after several passages (up to seven) the larger fraction of cells exhibited a marked astroglial phenotype independently of the growth factor (supplementary material Fig. S2D,E). Taken together, these data imply that the Tnc-expressing cells potentially constitute a subset of EGF-responsive gliogenic NPCs that emerges during early gliogenesis.

The loss of Tnc results in an increased proliferation of NPCs in vivo

The expression of Tnc by gliogenic NPCs prompted us to examine whether the loss of Tnc leads to alterations in proliferation rates in vivo. Therefore, we injected BrdU into time-pregnant mice at E14.5 and quantified the number of BrdU-positive cells after 24 hours in the spinal cord of wild-type (Fig. 3A) and Tnc-deficient (Fig. 3B) littermates. The loss of Tnc resulted in a small but significant increase in BrdU incorporation (wild type, 103±12.5; knockout, 121.3±8.3; $n=5$; $P=0.039$) (Fig. 3J). A closer inspection of the distribution of BrdU-positive cells within the spinal cord revealed that the number of BrdU-positive cells directly lining the
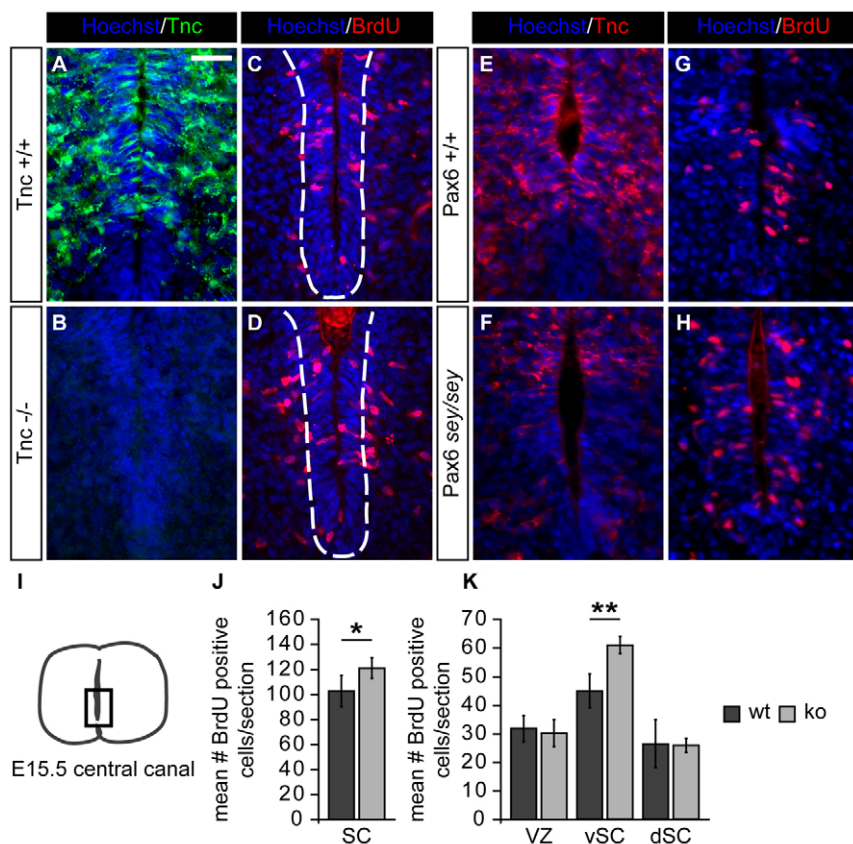

Fig. 3. BrdU incorporation analysis revealed an increased proliferation of NPCs in the Tnc-deficient spinal cord between E14.5 and E15.5. (A,B) Immunoreactivity for Tnc was strong around the central canal of the ventral spinal cord at E15.5 in wild-type tissue, except for the most ventral region. (C,D) To analyse the proliferation rate of NPCs in vivo, we injected BrdU intraperitoneally into pregnant mice at E14.5 and examined BrdU incorporation in the embryonic spinal cord 1 day later. In the Tnc-deficient tissue, we found more BrdU-positive cells, especially in the region with high Tnc immunoreactivity in wild-type sections. (E,F) We also noticed a reduced Tnc expression in the sey mutant spinal cord at E15.5. (G,H) Moreover, there was also an increased proliferation rate as assessed by BrdU incorporation in the region that exhibited a reduced Tnc expression. Scale bar: 25 μm. (I) Schematic of the area shown in A-H. (J,K) The quantification of BrdU-positive cells in the wild-type and Tnc-deficient tissue demonstrated that the loss of Tnc led to a significantly increased BrdU incorporation in the spinal cord (SC) ($n=5$, *$P=0.039$). A closer look at the distribution of BrdU-positive cells revealed that the number of BrdU-positive cells directly lining the central canal (VZ, ventricular zone) was not changed ($n=5$). Instead, the number of BrdU-positive cells in the ventral spinal cord, including the region next to the central canal (vSC) was significantly higher ($n=5$, **$P=0.0017$). Within the dorsal spinal cord (dSC), we did not observe any differences ($n=5$).

central canal was not changed (wild type, 31.9±4.6; knockout, 30.3±4.8; *n*=5) (Fig. 3K). However, there were significantly more BrdU-positive cells in the ventral spinal cord, including the region adjacent to the ventricular zone of Tnc-deficient animals in comparison with their wild-type littermates (wild type, 44.8±5.8; knockout, 60.7±3.0; *n*=5; *P*=0.001) (Fig. 3C,D,K). By contrast, the number of BrdU-positive cells in the dorsal spinal cord was not affected (wild type, 26.9±7.3; knockout, 26.1±2.3; *n*=5) (Fig. 3K). To further support the idea that the loss of Tnc leads to an increased proliferation rate during early gliogenesis in the spinal cord, we examined the Pax6 *sey* mutant mouse, the radial glia cells of which exhibit a reduced Tnc expression level during forebrain development (Gotz et al., 1998). Interestingly, the lack of Pax6 function results in an increased BrdU incorporation rate during early gliogenesis in the developing spinal cord (Sakurai and Osumi, 2008). Here, we demonstrate that mutated Pax6 also led to a reduced Tnc expression level in the spinal cord at E15.5 (Fig. 3E,F). Moreover, we could confirm the increased BrdU incorporation rate at that age (Fig. 3G,H). Taken together, we observed an increased proliferation rate during early gliogenesis in two independent mouse strains that lack Tnc in the developing spinal cord.

Tnc-deficiency leads to a sustained proliferation and delayed migration of immature astrocytes

To determine the fate of the newborn cells between E14.5 and E15.5, we combined in situ hybridisation for the immature astrocyte marker *Fgfr3* with the immunohistochemical detection of BrdU. We found that most if not all of the BrdU-positive cells around the central canal of the ventral spinal cord co-expressed the early astrocyte marker *Fgfr3*, suggesting a sustained generation of immature astrocytes in the absence of Tnc (Fig. 4A-C). Next, we took a closer look at the overall expression pattern of the Fgfr3. Although in the wild-type spinal cord, a substantial number of *Fgfr3*-expressing cells resided in the prospective ventral white matter, this population was

significantly smaller in the absence of Tnc [wild type, 15.7±1.6; knockout, 6.3±0.3; *P*=0.0006 (*n*=3)] (Fig. 4D-F). By contrast, we did not find any differences in the number or distribution of platelet-derived growth factor receptor alpha (*Pdgfra*)-expressing oligodendrocyte precursor cells [wild type, 172.5±23.3; knockout, 161.5±4.9 (*n*=2)] (Fig. 4G-I). We did also not observe any changes in the number of Sox2- or nestin-positive NPCs (supplementary material Fig. S3A,B) or of βIII-tubulin-positive neurons (data not shown). However, there seemed to be more NF1α-positive cells in the mutant spinal cord. But this difference was not significant (supplementary material Fig. S3A,B). Based on these results, we conclude that the loss of Tnc function not only leads to an increased generation but also to a delayed migration of immature astrocytes towards the pial membrane.

Tnc-deficiency affects the number of GFAP-positive astrocytes at the end of embryogenesis

Our data so far indicated that the early astrocyte lineage progression was delayed in the absence of Tnc. Therefore, we asked whether the loss of Tnc also leads to expression changes of the more mature astrocyte marker GFAP. First, we analysed the GFAP expression in the wild-type and Tnc-deficient spinal cord immunohistochemically at E18.5. Strikingly, we observed significantly more GFAP-positive cell processes in the ventral white matter in the Tnc-deficient in comparison with the wild-type spinal cord [wild type, 34.5±1.3 (*n*=3); knockout, 40.4±1.4 (*n*=2); *P*=0.017] (Fig. 5A-D), reflecting the increased generation of immature astrocytes earlier in development. This difference was, however, no longer visible within the young adult (P40) spinal cord (Fig. 5E,F). Next, we determined the number of GFAP-positive cells in Tnc-deficient and heterozygous littermates at E18.5. Consistent with the increased number of GFAP-positive cell processes, we observed a significantly increased number of GFAP-positive cells in the absence of Tnc [heterozygous, 6.1±0.3% (*n*=4); knockout, 10.8±0.6% (*n*=5); *P*<0.001] (Fig. 5G-I). Based on these
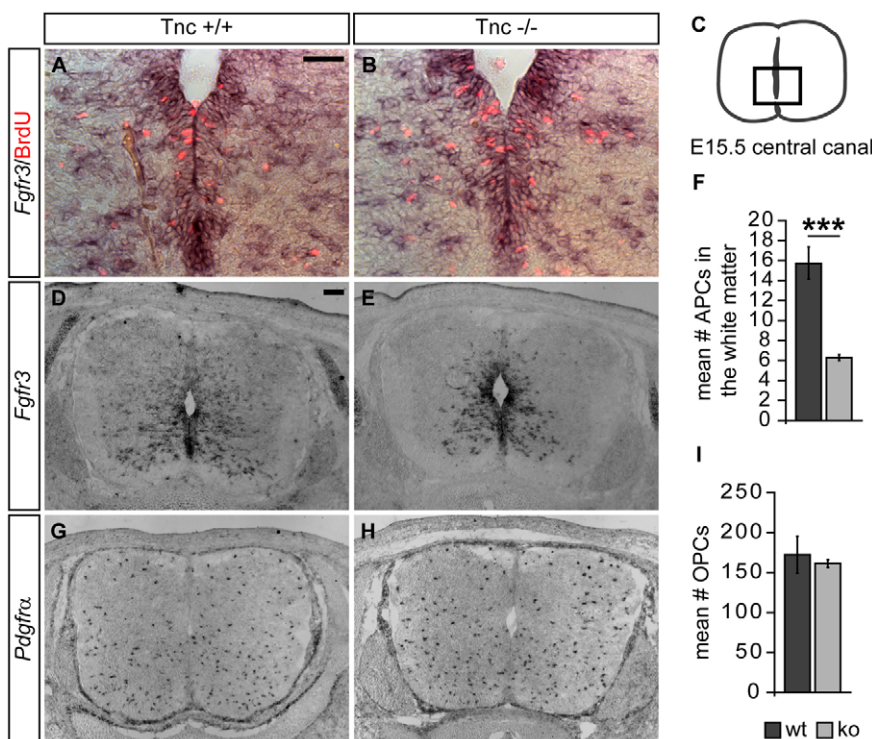

Fig. 4. Tnc deficiency leads to a sustained proliferation and delayed migration of immature astrocytes. (**A**,**B**) In situ hybridisation for the early astrocyte marker *Fgfr3* and immunhistochemical labelling of BrdU-positive cells showed that nearly all newborn cells between E14.5 and E15.5 are *Fgfr3*-expressing cells. Note, that this population is larger in the absence of Tnc. (**C**) Graphical depiction of the spinal cord region shown in A and B. (**D-F**) Photomicrographs of in situ hybridisation for *Fgfr3*, showing the migration of immature astrocytes from the central canal towards the pial membrane in wild-type and Tnc-deficient tissue (D,E). Whereas a considerable number of cells has already reached the prospective ventral white matter in the wild-type spinal cord, the migration of cells is significantly delayed in the absence of Tnc (*n*=3, ***P*=0.0006) (F). (**G-I**) By contrast, neither the number nor the distribution of *Pdgfra*-expressing oligodendrocyte precursor cells is changed. Scale bars: 25 μm in A,B; 50 μm in D,E,G,H.
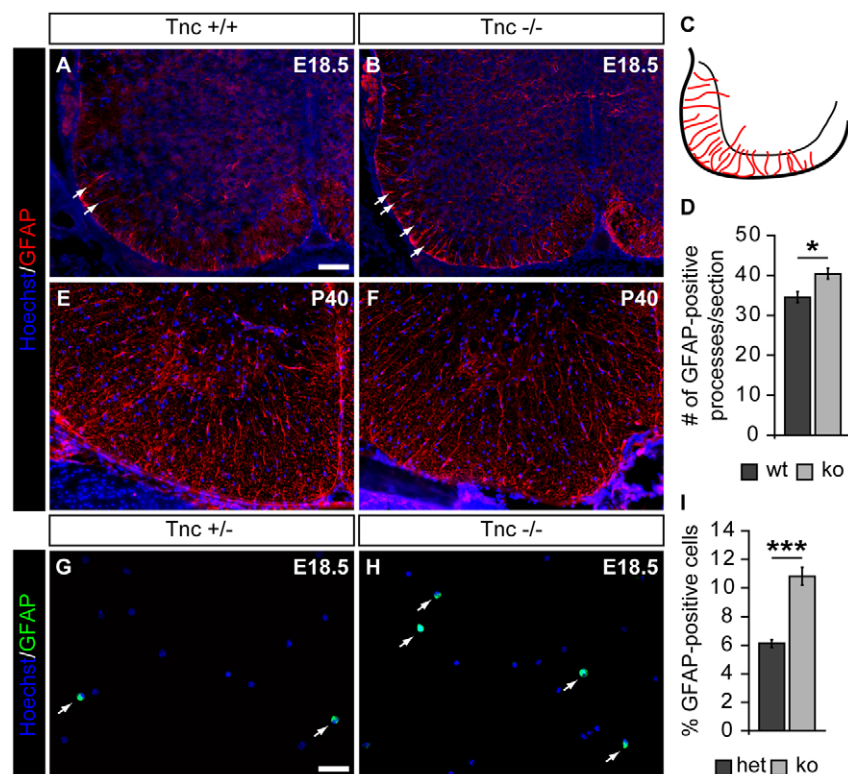
Fig. 5. Tnc deficiency leads to an increase in GFAP-positive cells in vivo.
(**A-D**) Immunohistochemical detection of GFAP in vivo at E18.5 (A,B) revealed that the loss of Tnc led to a significantly increased number of GFAP-positive cell processes (red in C) in the ventral white matter in comparison with wild-type littermates (white arrows) (wild type, n=3; knockout, n=2; *P=0.017) (D). (**E,F**) This difference was not longer observable in the adult spinal cord at P40.
(**G-I**) Immunohistochemical detection of GFAP in acutely dissociated E18.5 spinal cord cells from heterozygous and Tnc-deficient embryos revealed an increased number of GFAP-positive cells (white arrows in G and H) in the absence of Tnc (heterozygous, n=4; knockout, n=5; ***P<0.001). Scale bars: 100 μm in A,B,E,F; 50 μm in G,H.

data, we assume that the increased generation of immature astrocytes initially leads to an increased number of GFAP-positive cells in vivo.

Global gene expression changes in the absence of Tnc in vivo

In order to gain insight into potential mechanisms underlying the observed phenotypes in vivo, we performed a microarray analysis of E15.5 wild-type and Tnc-deficient spinal cords. Using the criteria mentioned in the Materials and methods, we initially found several known astrocyte enriched genes (Cahoy et al., 2008) (supplementary material Fig. S4A). Interestingly, we also observed an upregulation of sulfatase 1 (*Sulf1*) and sulfatase modifying factor 1 (*Sumf1*) (supplementary material Fig. S4B). Both genes directly intervene in FGF signalling (Buono et al., 2010; Otsuki et al., 2010). Moreover, we identified several genes that are involved in neural patterning during spinal cord development (supplementary material Fig. S4C). Using conventional RT-PCR, we additionally confirmed the upregulation of *Sulf1* and *Nkx2.2* (supplementary material Fig. S4D,E). Then, we analysed the expression pattern of *Sulf1*, *Nkx2.2*, *Nkx6.1* and *Pax6* around the ventral aspect of the central canal (Fig. 6A). In the absence of Tnc, we observed significantly more Nkx2.2-positive cells [wild type, 123.9±3.0; knockout, 149.0±5.5 (P=0.002; n=3)] (Fig. 6B,D). In addition, there was also a small population of Nkx2.2-positive cells above the canonical Nkx2.2-positive progenitor domain (white arrows in Fig. 6D). Two other examples of shifts in the territories of gene expression within the VZ were seen in the absence of Tnc. First, *Sulf1* expression was strongly enhanced in the presumptive VA3 domain (Fig. 6F). Second, in line with the microarray data, we also documented an increased number of Nkx6.1-positive cells in the Tnc-deficient spinal cord (wild type, 142.8±12.0 (n=4); knockout, 173.6±5.7 (n=3) (P=0.036)] (Fig. 6C,E) and, strikingly,

the expression territory of Nkx6.1 extended into the VA1 domain (Fig. 6E). By contrast, the expression of Pax6 was not changed (Fig. 6G).

Tnc-deficiency leads to alterations in growth factor responsiveness

Sulf1 is a downstream target of Nkx2.2 (Genethliou et al., 2009) and is expressed in the developing ventral spinal cord during the neuron-to-glia switch (Ratzka et al., 2010). Furthermore, Sulf1 influences both FGF and bone morphogenetic protein (BMP) signalling (Lamanna et al., 2008; Otsuki et al., 2010). Thus, we hypothesized that the increased *Sulf1* expression in the Tnc-deficient spinal cord may lead to alterations in growth factor responsiveness. To test this interpretation, we again performed neurosphere formation assays. After 1 week, we observed a significantly reduced EGF-dependent neurosphere formation from E15.5 Tnc-deficient spinal cord cells [wild type EGF, 248.8±75.8 (n=13); knockout EGF, 172.8±34.6 (n=6); P=0.035]. This difference was, however, not longer detectable at E18.5 [wild type EGF, 50.0±20.4 (n=4); knockout EGF, 48.3±9.0; P=0.56] (Fig. 7A). In line with these data, immunohistochemical detection of the EGFR at E15.5 showed less EGFR immunoreactivity in the Tnc-deficient spinal cord (Fig. 7B). By contrast, the number of neurospheres grown in the presence of FGF2 was not changed for either E15.5 [wild type FGF2, 280.5±76.3 (n=10); knockout FGF2, 250.3±68.3 (n=6); P=0.440] or E18.5 [wild type FGF2, 75.0±16.7 (n=4); knockout FGF2, 88.2±23.1 (n=6); P=0.39] spinal cord cells (Fig. 7A). However, neurospheres grown from Tnc-deficient cells in the presence of FGF2 exhibited a significantly larger diameter in comparison with wild-type cells (supplementary material Fig. S5).

The observed impact of Tnc on EGF responsiveness raised the issue of whether it would be possible to drive an EGF-dependent neurosphere formation by adding affinity-purified Tnc. To
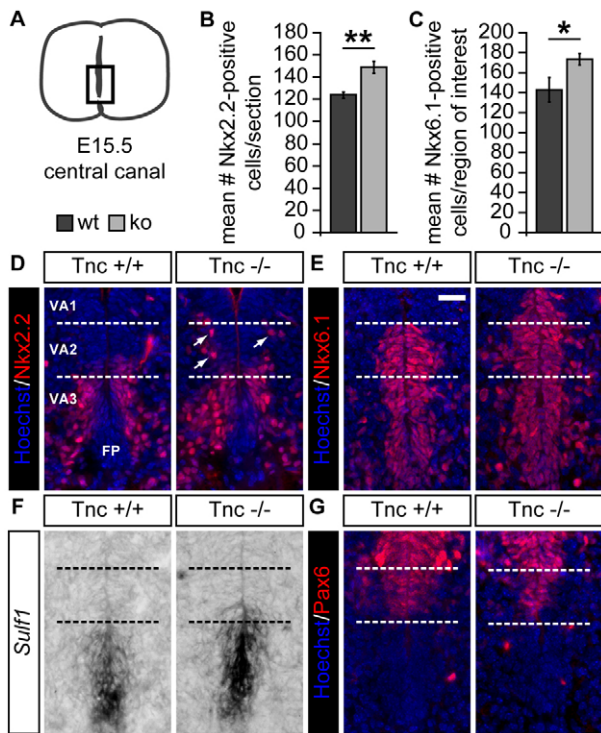
Fig. 6. The patterning of astrocyte progenitor domains is altered in the Tnc-deficient spinal cord. (**A**) Based on our microarray data, we histologically analysed the expression of the homeodomain transcription factors Nkx2.2, Nkx6.1 and Pax6, and of Sulf1 around the ventral aspect of the central canal at E15.5. (**B-E**) Immunohistochemical detection of Nkx2.2 revealed a small ectopic Nkx2.2-positive cell population within the VA2 domain in the Tnc-deficient spinal cord (D,E). Moreover, the total number of Nkx2.2-positive cells was significantly increased (wild type, $n=3$; knockout, $n=3$; **$P=0.002$) (B). The number of Nkx6.1-positive cells was also significantly higher (wild type, $n=4$; knockout, $n=3$; *$P=0.036$) (C). Strikingly, the Nkx6.1-positive cells extended into the VA1 domain. (**F**) In situ hybridisation for Sulf1 demonstrated that it is mainly expressed in the floor plate and to less extent in the VA3 domain. However, Sulf1 becomes upregulated within this domain in the absence of Tnc. (**G**) In contrast to Nkx2.2 and Nkx6.1, the expression of Pax6 was not changed in the Tnc-deficient spinal cord. Broken lines indicate the borders between VA1-VA3. VA1-VA3, ventral astrocyte progenitor domains 1-3; FP, floor plate. Scale bar: 25 µm.

Fig. 7. Tnc regulates growth factor responsiveness during gliogenesis in the developing spinal cord. (**A**) In the absence of Tnc, EGF responsiveness was reduced at E15.5 in the spinal cord, as revealed by neurosphere formation assays (wild type, $n=13$; knockout, $n=6$; *$P=0.035$). However, at E18.5 we no longer observed differences in EGF responsiveness (wild type, $n=4$; knockout, $n=6$). The number of neurospheres grown in the presence of FGF2 was not different for both ages. (**B**) Immunohistochemical detection of the EGFR demonstrated a reduced EGFR immunoreactivity in the mutant tissue. In particular, the region around the ventral central canal exhibited less EGFR immunoreactivity. (**C,D**) The addition of Tnc to wild-type E13.5 spinal cord cells significantly enhanced an EGF-dependent neurosphere formation (*$P=0.033$). At the same time, it strongly suppressed the formation of neurospheres in the presence of FGF2 (***$P=0.0002$). Scale bar: 25 µm.

investigate this, we cultivated E13.5 wild-type spinal cord cells in the presence of either EGF (5 ng/ml) or FGF2 (5 ng/ml) and added either purified Tnc (5 µg/ml) or PBS as control (Fig. 7C). We found that the addition of Tnc significantly affected the number of forming neurospheres under both growth factor conditions, leading to either more neurospheres in the presence of EGF [PBS 39.0±17.5; Tnc 51.0±19.9; $P=0.033$ ($n=4$)] or to fewer neurospheres in the presence of FGF2 [PBS, 107.5±12.9; Tnc, 79.3±15.3; $P<0.001$ ($n=4$)] (Fig. 7D). Based on these neurosphere data, we conclude that Tnc regulates growth factor responsiveness during spinal cord development.

DISCUSSION

Tnc becomes upregulated upon spinal cord lesion by reactive astrocytes and influences the regenerative capacity of the damaged tissue (Camand et al., 2004; Chen et al., 2010; Dobbertin et al., 2010). However, the functions of Tnc during spinal cord
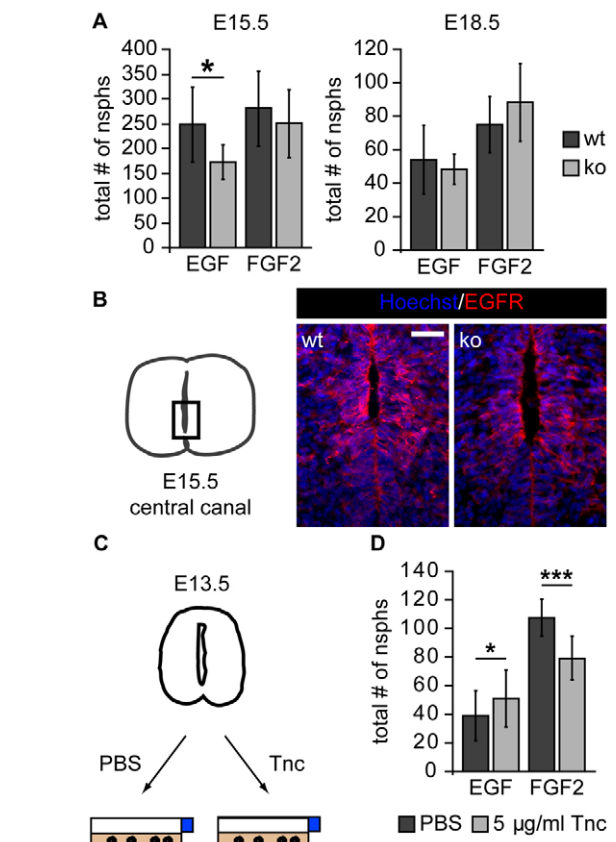
development so far remained elusive. Here, we could show that Tnc is expressed within the astroglial lineage during late embryonic spinal cord development. We provide evidence for an enhanced proliferation and delayed migration of presumptive immature astrocytes towards the prospective ventral white matter in the Tnc-deficient spinal cord. We also documented an increased number of GFAP-positive cells in vivo at the end of embryonic development. The loss of Tnc leads to an upregulation of Nkx6.1, Nkx2.2 and its downstream target Sulf1. Sulf1 interferes with both sonic hedgehog (Shh), and FGF-signalling owing to its ability to cleave sulphate residues from heparan sulphate proteoglycans (Danesin et al., 2006; Lamanna et al., 2008). Along these lines, we observed alterations in the FGF2 and EGF responsiveness of Tnc-deficient spinal cord NPCs.

It is known that there are at least three different astrocyte subpopulations in the embryonic mouse spinal cord defined by the combinatorial expression of the homeodomain transcription factors

Pax6 and Nkx6.1 within the VZ progenitor domains (VA1-VA3) and in the ventral white matter (Hochstim et al., 2008). We believe that the secreted ECM molecule Tnc is involved in establishing and/or maintaining these domains during early gliogenesis. Tnc is specifically expressed in the VA1 and VA2 domains. Both domains contain Pax6-positive cells, whereas the latter also contains Nkx6.1-positive cells. By contrast, the VA3 domain harbours Nkx6.1-, Nkx2.2- and Sulf1-expressing cells (Fig. 8A). In the absence of Tnc, the VA2 domain expands dorsally (Fig. 8B). The cross-repressive interactions of Pax6 and Nkx2.2 (Briscoe et al., 1999; Ericson et al., 1997) may be the reason why the VZ of the VA2 domain does not express Nkx2.2 in the absence of Tnc. Instead some ectopic Nkx2.2-positive cells appear in the marginal zone. Because Sulf1 is a known downstream target of Nkx2.2 (Genethliou et al., 2009), it is plausible that Sulf1 also becomes upregulated. However, this upregulation is confined only to the VA3 domain. Interestingly, both Nkx2.2 and Sulf1 expand dorsally in the Pax6 *sey* mutant spinal cord (Genethliou et al., 2009; Sugimori et al., 2007), where we found a reduced Tnc expression. The domain shift is most probably due to modified Shh signalling. Interestingly, we found that, as well as Sulf1, the glycoprotein vitronectin is also upregulated. Both molecules promote Shh signalling in the developing ventral spinal cord (Danesin et al., 2006; Martinez-Morales et al., 1997).

Sulf1 also negatively regulates FGF signalling (Lamanna et al., 2008; Otsuki et al., 2010). Low FGF-signalling levels during early forebrain development lead to proliferation of NPCs, whereas high levels lead to an upregulation of the EGFR and consequently to the onset of gliogenesis (Lillien and Raphael, 2000; Qian et al., 1997; Temple, 2001). Given that this concept holds also true for spinal cord NPCs, an upregulation of Sulf1 in the absence of Tnc should attenuate FGF signalling and lead to a delayed EGF responsiveness. Indeed, we found a transiently decreased EGF responsiveness in vivo at the onset of gliogenesis. In addition, we were able to induce EGF-responsiveness in E13.5 wild-type spinal

cord NPCs by adding purified Tnc. Consistent with this, Tnc regulates the EGFR expression in telencephalic NPCs (Garcion et al., 2004; Yagi et al., 2010). Considering our own unpublished observations that the overall proliferation level measured as the number of phospho histone H3-positive cells at the onset of gliogenesis is relatively low, we assumed that strong EGF responsiveness during gliogenesis might regulate cell migration rather than cell proliferation. An EGF-dependent migration of NPCs and astrocytes during forebrain development has already been shown (Caric et al., 2001). Moreover, the EGF-like domains of Tnc can bind to the EGFR (Iyer et al., 2007) and promote the migration rather than the proliferation of cultured fibroblasts (Iyer et al., 2008). The fact that the migration of *Fgfr3*-expressing cells is delayed at the same time when EGF responsiveness is reduced in the absence of Tnc strongly supports our idea.

According to the model that low FGF-signalling levels during early development foster proliferation the loss of Tnc should result in a sustained proliferation of NPCs at the onset of gliogenesis. Indeed, we observed an increased BrdU incorporation in the Tnc-deficient spinal cord. Likewise, Tnc-deficient neurospheres grown in the presence of FGF2 were significantly larger than wild-type neurospheres, and we were able to suppress the FGF2-dependent neurosphere formation by adding purified Tnc to E13.5 spinal cord cells. Finally, we could also confirm an increased BrdU incorporation in the *sey* mutant spinal cord (Sakurai and Osumi, 2008), which exhibits a reduced Tnc expression level.

Among the additional BrdU-positive cells in the Tnc-deficient spinal cord, the great majority expressed *Fgfr3*, suggesting a sustained generation of immature astrocytes. Moreover, the microarray analysis revealed a moderate upregulation of the *Fgfr3* as well as of the known astrocyte specific genes *Slc14a1*, *Aqp4*, *Slc25a18* and *Maob* (Cahoy et al., 2008; Nagelhus et al., 2004). Interestingly, even *Olig2* is expressed in the astroglial lineage and regulates white-matter astrocyte development (Cai et al., 2007; Masahira et al., 2006). Thus, Tnc appears to induce a quiescent
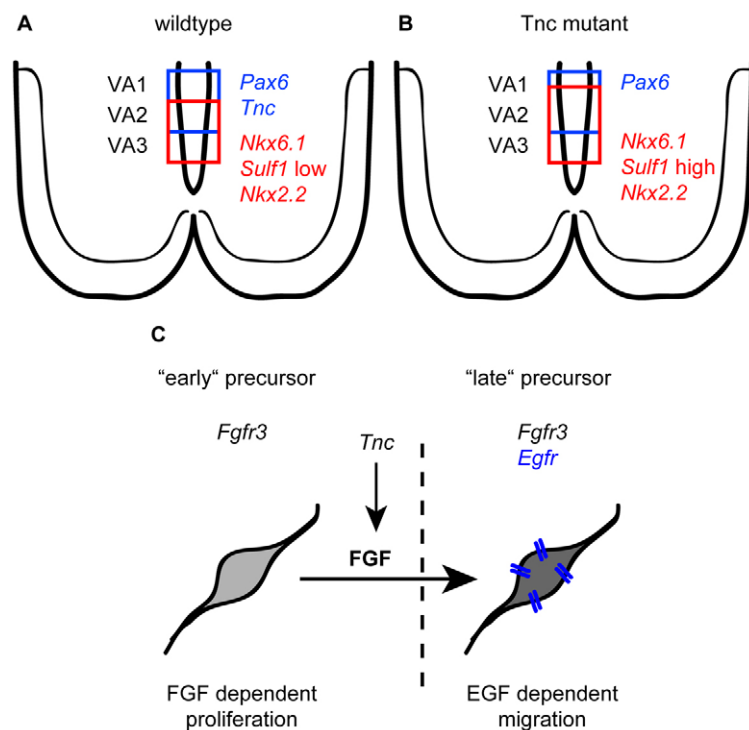

Fig. 8. Model for the role of Tnc during embryonic spinal cord development. (**A**) Concerning the transcription factors Pax6 and Nkx6.1, three separate progenitor cell domains (VA1-VA3) exist at early gliogenesis in the ventral wild-type spinal cord: a dorsal Pax6-positive domain (VA1) (blue), a more ventral Pax6-/Nkx2.2-positive domain (VA2) (overlap between blue and red) and an even more ventral Nkx6.1-positive domain (VA3) (red). Tnc is expressed in the VA1 and VA2 domains. By contrast, Nkx2.2 and Sulf1 are expressed in the VA3 domain. (**B**) In the absence of Tnc, the VA2 domain expands dorsally into the VA1 domain. Moreover, several Nkx2.2-positive cells appear around the VA2 domain, and the expression of Sulf1 within the VA3 domain increases, potentially leading to alterations in FGF responsiveness. (**C**) Changes in FGF responsiveness at the onset of gliogenesis affect the transition of FGF-responsive early precursor cells into late FGF/EGF-responsive precursor cells. It is believed that this transition takes place as soon as FGF signalling reaches a threshold (broken line). Although the former cell population undergoes a FGF-dependent proliferation, the latter population most probably undergoes an EGF-dependent migration. Based on our data, Tnc positively regulates FGF responsiveness and thus the above-mentioned transition. The loss of Tnc, therefore, leads to a sustained proliferation and delayed migration.

state of spinal cord astroglial cells. We propose that the increased BrdU incorporation at early gliogenesis is due to a prolonged FGF-dependent proliferation of *Fgfr3*-expressing cells, most likely being immature astrocytes. However, it is hard to define that cell type exactly, as the majority of markers (e.g. NF1α, NF1β, Fgfr3, glutamine synthethase and S100β), which are usually used to identify early astroglial cells, are expressed by astroglial progenitor cells in the VZ and by immature astrocytes migrating into the MZ (Deneen et al., 2006; Sugimori et al., 2007; Young et al., 2010). Yet, consistent with our interpretation, Tnc suppresses the proliferation of adult cultured human astrocytes (Holley et al., 2005). Moreover, we documented an increased number of GFAP-positive cells and cell processes in the ventral white matter at E18.5. The latter was no longer observable in the adult spinal cord. However, Tnc-dependent GFAP expression level changes under pathological conditions have already been reported (Kazanis et al., 2007; Steindler et al., 1995). Therefore, it is conceivable that the absence of Tnc might also affect proliferation and migration of at least some reactive astrocytes under these conditions. As reactive astrocytes are currently considered to display stem cell characteristics (Robel et al., 2011), investigating the regulatory functions of Tnc on these cells would be of great interest. Nevertheless, whether the total number of astrocytes in the adult spinal cord is altered remains to be investigated. In this context, it is noteworthy that both the cortex (Irintchev et al., 2005) and the hippocampus (Gurevicius et al., 2009) of adult Tnc-deficient animals contain more S100β-positive astrocytes in comparison with wild-type littermates. These phenotypes are in accordance with an increased generation of astrocytes during development.

Based on the model of an early FGF-responsive and a late FGF/EGF-responsive NPC (Lillien and Raphael, 2000), we propose that also in the embryonic spinal cord early NPCs undergo an FGF-dependent proliferation. As soon as FGF signalling reaches a certain threshold, this early NPC switches into a late FGF/EGF-responsive NPC. At that stage, NPCs stop proliferating and start migrating away from the VZ towards the prospective ventral white matter in an EGF-dependent manner (Fig. 8C). We believe that Tnc and other ECM molecules promote the timely transition from an early into a late NPC. Along these lines, we recently showed that interference with glycosaminoglycan biology strongly affects cortical NPC maturation (Sirko et al., 2010; Sirko et al., 2007). In the spinal cord, the loss of Tnc leads to a sustained FGF-dependent proliferation and delayed EGF-dependent migration of immature astrocytes caused by reduced FGF signalling levels, most probably resulting from an upregulation of *Sulf1*. To our knowledge, this is the first study that reports on a potential role of ECM molecules for the astroglial lineage progression during development and highlights the importance of the cellular micro-environment for the precise regulation of NPC behaviour.

References
Barres, B. A. (2008). The mystery and magic of glia: a perspective on their roles in health and disease. *Neuron* **60**, 430-440.

Barry, D. and McDermott, K. (2005). Differentiation of radial glia from radial precursor cells and transformation into astrocytes in the developing rat spinal cord. *Glia* **50**, 187-197.

Briscoe, J., Sussel, L., Serup, P., Hartigan-O'Connor, D., Jessell, T. M., Rubenstein, J. L. and Ericson, J. (1999). Homeobox gene Nkx2.2 and specification of neuronal identity by graded Sonic hedgehog signalling. *Nature* **398**, 622-627.

Brodkey, J. A., Laywell, E. D., O'Brien, T. F., Faissner, A., Stefansson, K., Dorries, H. U., Schachner, M. and Steindler, D. A. (1995). Focal brain injury and upregulation of a developmentally regulated extracellular matrix protein. *J. Neurosurg.* **82**, 106-112.

Buono, M., Visigalli, I., Bergamasco, R., Biffi, A. and Cosma, M. P. (2010). Sulfatase modifying factor 1-mediated fibroblast growth factor signaling primes hematopoietic multilineage development. *J. Exp. Med.* **207**, 1647-1660.

Cahoy, J. D., Emery, B., Kaushal, A., Foo, L. C., Zamanian, J. L., Christopherson, K. S., Xing, Y., Lubischer, J. L., Krieg, P. A., Krupenko, S. A. et al. (2008). A transcriptome database for astrocytes, neurons, and oligodendrocytes: a new resource for understanding brain development and function. *J. Neurosci.* **28**, 264-278.

Cai, J., Chen, Y., Cai, W. H., Hurlock, E. C., Wu, H., Kernie, S. G., Parada, L. F. and Lu, Q. R. (2007). A crucial role for Olig2 in white matter astrocyte development. *Development* **134**, 1887-1899.

Camand, E., Morel, M. P., Faissner, A., Sotelo, C. and Dusart, I. (2004). Long-term changes in the molecular composition of the glial scar and progressive increase of serotoninergic fibre sprouting after hemisection of the mouse spinal cord. *Eur. J. Neurosci.* **20**, 1161-1176.

Caric, D., Raphael, H., Viti, J., Feathers, A., Wancio, D. and Lillien, L. (2001). EGFRs mediate chemotactic migration in the developing telencephalon. *Development* **128**, 4203-4216.

Chen, J., Joon Lee, H., Jakovcevski, I., Shah, R., Bhagat, N., Loers, G., Liu, H. Y., Meiners, S., Taschenberger, G., Kugler, S. et al. (2010). The extracellular matrix glycoprotein Tenascin-C is beneficial for spinal cord regeneration. *Mol. Ther.* **18**, 1769-1777.

Coles-Takabe, B. L., Brain, I., Purpura, K. A., Karpowicz, P., Zandstra, P. W., Morshead, C. M. and van der Kooy, D. (2008). Don't look: growing clonal versus nonclonal neural stem cell colonies. *Stem Cells* **26**, 2938-2944.

Czopka, T., Von Holst, A., Schmidt, G., Ffrench-Constant, C. and Faissner, A. (2009). Tenascin C and tenascin R similarly prevent the formation of myelin membranes in a RhoA-dependent manner, but antagonistically regulate the expression of myelin basic protein via a separate pathway. *Glia* **57**, 1790-1801.

Czopka, T., von Holst, A., ffrench-Constant, C. and Faissner, A. (2010). Regulatory mechanisms that mediate tenascin C-dependent inhibition of oligodendrocyte precursor differentiation. *J. Neurosci.* **30**, 12310-12322.

Danesin, C., Agius, E., Escalas, N., Ai, X., Emerson, C., Cochard, P. and Soula, C. (2006). Ventral neural progenitors switch toward an oligodendroglial fate in response to increased Sonic hedgehog (Shh) activity: involvement of Sulfatase 1 in modulating Shh signaling in the ventral spinal cord. *J. Neurosci.* **26**, 5037-5048.

Deneen, B., Ho, R., Lukaszewicz, A., Hochstim, C. J., Gronostajski, R. M. and Anderson, D. J. (2006). The transcription factor NFIA controls the onset of gliogenesis in the developing spinal cord. *Neuron* **52**, 953-968.

Dobbertin, A., Czvitkovich, S., Theocharidis, U., Garwood, J., Andrews, M. R., Properzi, F., Lin, R., Fawcett, J. W. and Faissner, A. (2010). Analysis of combinatorial variability reveals selective accumulation of the fibronectin type III domains B and D of tenascin-C in injured brain. *Exp. Neurol.* **225**, 60-73.

Ericson, J., Rashbass, P., Schedl, A., Brenner-Morton, S., Kawakami, A., van Heyningen, V., Jessell, T. M. and Briscoe, J. (1997). Pax6 controls progenitor cell identity and neuronal fate in response to graded Shh signaling. *Cell* **90**, 169-180.

Faissner, A. and Kruse, J. (1990). J1/tenascin is a repulsive substrate for central nervous system neurons. *Neuron* **5**, 627-637.

Faissner, A., Pyka, M., Geissler, M., Sobik, T., Frischknecht, R., Gundelfinger, E. D. and Seidenbecher, C. (2010). Contributions of astrocytes to synapse formation and maturation-Potential functions of the perisynaptic extracellular matrix. *Brain Res. Rev.* **63**, 26-38.

Forsberg, E., Hirsch, E., Frohlich, L., Meyer, M., Ekblom, P., Aszodi, A., Werner, S. and Fassler, R. (1996). Skin wounds and severed nerves heal normally in mice lacking tenascin-C. *Proc. Natl. Acad. Sci. USA* **93**, 6594-6599.

Garcion, E., Halilagic, A., Faissner, A. and ffrench-Constant, C. (2004). Generation of an environmental niche for neural stem cell development by the extracellular matrix molecule tenascin C. *Development* **131**, 3423-3432.

Garwood, J., Garcion, E., Dobbertin, A., Heck, N., Calco, V., ffrench-Constant, C. and Faissner, A. (2004). The extracellular matrix glycoprotein Tenascin-C is expressed by oligodendrocyte precursor cells and required for the regulation of maturation rate, survival and responsiveness to platelet-derived growth factor. *Eur. J. Neurosci.* **20**, 2524-2540.

Genethliou, N., Panayiotou, E., Panayi, H., Orford, M., Mean, R., Lapathitis, G. and Malas, S. (2009). Spatially distinct functions of PAX6 and NKX2.2 during gliogenesis in the ventral spinal cord. *Biochem. Biophys. Res. Commun.* **382**, 69-73.

Gentleman, R. C., Carey, V. J., Bates, D. M., Bolstad, B., Dettling, M., Dudoit, S., Ellis, B., Gautier, L., Ge, Y., Gentry, J. et al. (2004). Bioconductor: open software development for computational biology and bioinformatics. *Genome Biol.* **5**, R80.

Gotz, M., Stoykova, A. and Gruss, P. (1998). Pax6 controls radial glia differentiation in the cerebral cortex. *Neuron* **21**, 1031-1044.

Gurevicius, K., Kuang, F., Stoenica, L., Irintchev, A., Gureviciene, I., Dityatev, A., Schachner, M. and Tanila, H. (2009). Genetic ablation of tenascin-C expression leads to abnormal hippocampal CA1 structure and electrical activity in vivo. *Hippocampus* **19**, 1232-1246.

Haydon, P. G. (2001). GLIA: listening and talking to the synapse. *Nat. Rev. Neurosci.* **2**, 185-193.

Hochstim, C., Deneen, B., Lukaszewicz, A., Zhou, Q. and Anderson, D. J. (2008). Identification of positionally distinct astrocyte subtypes whose identities are specified by a homeodomain code. *Cell* **133**, 510-522.

Holley, J. E., Gveric, D., Whatmore, J. L. and Gutowski, N. J. (2005). Tenascin C induces a quiescent phenotype in cultured adult human astrocytes. *Glia* **52**, 53-58.

Irintchev, A., Rollenhagen, A., Troncoso, E., Kiss, J. Z. and Schachner, M. (2005). Structural and functional aberrations in the cerebral cortex of tenascin-C deficient mice. *Cereb. Cortex* **15**, 950-962.

Irizarry, R. A., Hobbs, B., Collin, F., Beazer-Barclay, Y. D., Antonellis, K. J., Scherf, U. and Speed, T. P. (2003). Exploration, normalization, and summaries of high density oligonucleotide array probe level data. *Biostatistics* **4**, 249-264.

Iyer, A. K., Tran, K. T., Borysenko, C. W., Cascio, M., Camacho, C. J., Blair, H. C., Bahar, I. and Wells, A. (2007). Tenascin cytotactin epidermal growth factor-like repeat binds epidermal growth factor receptor with low affinity. *J. Cell. Physiol.* **211**, 748-758.

Iyer, A. K., Tran, K. T., Griffith, L. and Wells, A. (2008). Cell surface restriction of EGFR by a tenascin cytotactin-encoded EGF-like repeat is preferential for motility-related signaling. *J. Cell. Physiol.* **214**, 504-512.

Kazanis, I., Belhadi, A., Faissner, A. and Ffrench-Constant, C. (2007). The adult mouse subependymal zone regenerates efficiently in the absence of tenascin-C. *J. Neurosci.* **27**, 13991-13996.

Lamanna, W. C., Frese, M. A., Balleininger, M. and Dierks, T. (2008). Sulf loss influences N-, 2-O-, and 6-O-sulfation of multiple heparan sulfate proteoglycans and modulates fibroblast growth factor signaling. *J. Biol. Chem.* **283**, 27724-27735.

Laywell, E. D., Dorries, U., Bartsch, U., Faissner, A., Schachner, M. and Steindler, D. A. (1992). Enhanced expression of the developmentally regulated extracellular matrix molecule tenascin following adult brain injury. *Proc. Natl. Acad. Sci. USA* **89**, 2634-2638.

Lillien, L. and Raphael, H. (2000). BMP and FGF regulate the development of EGF-responsive neural progenitor cells. *Development* **127**, 4993-5005.

Martinez-Morales, J. R., Barbas, J. A., Marti, E., Bovolenta, P., Edgar, D. and Rodriguez-Tebar, A. (1997). Vitronectin is expressed in the ventral region of the neural tube and promotes the differentiation of motor neurons. *Development* **124**, 5139-5147.

Masahira, N., Takebayashi, H., Ono, K., Watanabe, K., Ding, L., Furusho, M., Ogawa, Y., Nabeshima, Y., Alvarez-Buylla, A., Shimizu, K. et al. (2006). Olig2-positive progenitors in the embryonic spinal cord give rise not only to motoneurons and oligodendrocytes, but also to a subset of astrocytes and ependymal cells. *Dev. Biol.* **293**, 358-369.

Muroyama, Y., Fujiwara, Y., Orkin, S. H. and Rowitch, D. H. (2005). Specification of astrocytes by bHLH protein SCL in a restricted region of the neural tube. *Nature* **438**, 360-363.

Nagelhus, E. A., Mathiisen, T. M. and Ottersen, O. P. (2004). Aquaporin-4 in the central nervous system: cellular and subcellular distribution and coexpression with KIR4.1. *Neuroscience* **129**, 905-913.

Otsuki, S., Hanson, S. R., Miyaki, S., Grogan, S. P., Kinoshita, M., Asahara, H., Wong, C. H. and Lotz, M. K. (2010). Extracellular sulfatases support cartilage homeostasis by regulating BMP and FGF signaling pathways. *Proc. Natl. Acad. Sci. USA* **107**, 10202-10207.

Pringle, N. P., Yu, W. P., Guthrie, S., Roelink, H., Lumsden, A., Peterson, A. C. and Richardson, W. D. (1996). Determination of neuroepithelial cell fate: induction of the oligodendrocyte lineage by ventral midline cells and sonic hedgehog. *Dev. Biol.* **177**, 30-42.

Pringle, N. P., Yu, W. P., Howell, M., Colvin, J. S., Ornitz, D. M. and Richardson, W. D. (2003). Fgfr3 expression by astrocytes and their precursors: evidence that astrocytes and oligodendrocytes originate in distinct neuroepithelial domains. *Development* **130**, 93-102.

Qian, X., Davis, A. A., Goderie, S. K. and Temple, S. (1997). FGF2 concentration regulates the generation of neurons and glia from multipotent cortical stem cells. *Neuron* **18**, 81-93.

Ratzka, A., Mundlos, S. and Vortkamp, A. (2010). Expression patterns of sulfatase genes in the developing mouse embryo. *Dev. Dyn.* **239**, 1779-1788.

Represa, A., Shimazaki, T., Simmonds, M. and Weiss, S. (2001). EGF-responsive neural stem cells are a transient population in the developing mouse spinal cord. *Eur. J. Neurosci.* **14**, 452-462.

Robel, S., Mori, T., Zoubaa, S., Schlegel, J., Sirko, S., Faissner, A., Goebbels, S., Dimou, L. and Gotz, M. (2009). Conditional deletion of beta1-integrin in astroglia causes partial reactive gliosis. *Glia* **57**, 1630-1647.

Robel, S., Berninger, B. and Gotz, M. (2011). The stem cell potential of glia: lessons from reactive gliosis. *Nat. Rev. Neurosci.* **12**, 88-104.

Rowitch, D. H., Lu, Q. R., Kessaris, N. and Richardson, W. D. (2002). An oligarchy rules neural development. *Trends Neurosci.* **25**, 417-422.

Sakurai, K. and Osumi, N. (2008). The neurogenesis-controlling factor, Pax6, inhibits proliferation and promotes maturation in murine astrocytes. *J. Neurosci.* **28**, 4604-4612.

Sirko, S., von Holst, A., Wizenmann, A., Gotz, M. and Faissner, A. (2007). Chondroitin sulfate glycosaminoglycans control proliferation, radial glia cell differentiation and neurogenesis in neural stem/progenitor cells. *Development* **134**, 2727-2738.

Sirko, S., Neitz, A., Mittmann, T., Horvat-Brocker, A., von Holst, A., Eysel, U. T. and Faissner, A. (2009). Focal laser-lesions activate an endogenous population of neural stem/progenitor cells in the adult visual cortex. *Brain* **132**, 2252-2264.

Sirko, S., von Holst, A., Weber, A., Wizenmann, A., Theocharidis, U., Gotz, M. and Faissner, A. (2010). Chondroitin sulfates are required for fibroblast growth factor-2-dependent proliferation and maintenance in neural stem cells and for epidermal growth factor-dependent migration of their progeny. *Stem Cells* **28**, 775-787.

Snow, D. M., Steindler, D. A. and Silver, J. (1990). Molecular and cellular characterization of the glial roof plate of the spinal cord and optic tectum: a possible role for a proteoglycan in the development of an axon barrier. *Dev. Biol.* **138**, 359-376.

Sommer, I. and Schachner, M. (1981). Monoclonal antibodies (O1 to O4) to oligodendrocyte cell surfaces: an immunocytological study in the central nervous system. *Dev. Biol.* **83**, 311-327.

Steindler, D. A., Settles, D., Erickson, H. P., Laywell, E. D., Yoshiki, A., Faissner, A. and Kusakabe, M. (1995). Tenascin knockout mice: barrels, boundary molecules, and glial scars. *J. Neurosci.* **15**, 1971-1983.

Stoykova, A., Fritsch, R., Walther, C. and Gruss, P. (1996). Forebrain patterning defects in small eye mutant mice. *Development* **122**, 3453-3465.

Stoykova, A., Gotz, M., Gruss, P. and Price, J. (1997). Pax6-dependent regulation of adhesive patterning, R-cadherin expression and boundary formation in developing forebrain. *Development* **124**, 3765-3777.

Sugimori, M., Nagao, M., Bertrand, N., Parras, C. M., Guillemot, F. and Nakafuku, M. (2007). Combinatorial actions of patterning and HLH transcription factors in the spatiotemporal control of neurogenesis and gliogenesis in the developing spinal cord. *Development* **134**, 1617-1629.

Talts, J. F., Wirl, G., Dictor, M., Muller, W. J. and Fassler, R. (1999). Tenascin-C modulates tumor stroma and monocyte/macrophage recruitment but not tumor growth or metastasis in a mouse strain with spontaneous mammary cancer. *J. Cell Sci.* **112**, 1855-1864.

Temple, S. (2001). The development of neural stem cells. *Nature* **414**, 112-117.

von Holst, A., Sirko, S. and Faissner, A. (2006). The unique 473HD-Chondroitinsulfate epitope is expressed by radial glia and involved in neural precursor cell proliferation. *J. Neurosci.* **26**, 4082-4094.

von Holst, A., Egbers, U., Prochiantz, A. and Faissner, A. (2007). Neural stem/progenitor cells express 20 tenascin C isoforms that are differentially regulated by Pax6. *J. Biol. Chem.* **282**, 9172-9181.

Yagi, H., Yanagisawa, M., Suzuki, Y., Nakatani, Y., Ariga, T., Kato, K. and Yu, R. K. (2010). HNK-1 epitope-carrying Tenascin-C spliced variant regulates the proliferation of mouse embryonic neural stem cells. *J. Biol. Chem.* **285**, 37293-37301.

Young, K. M., Mitsumori, T., Pringle, N., Grist, M., Kessaris, N. and Richardson, W. D. (2010). An Fgfr3-iCreER(T2) transgenic mouse line for studies of neural stem cells and astrocytes. *Glia* **58**, 943-953.

DEVELOPMENT